ME-NETT 25
The 25th Conference of the Mechanical Engineering Network of Thailand

CST06

The 25th Conference of the Mechanical Engineering Network of Thailand
October 19 – 21, 2011, Krabi

Control volume finite element method for thermal conduction analysis of a square plate subjected to non-uniform volumetric heat generation

Passakorn Vessakosol

Department of Mechanical Engineering, Faculty of Engineering, Prince of Songkla University, Songkla, Thailand 90110
E-mail: passakorn_v@yahoo.com, Tel. 074 287035-6, Fax. 074 558 830

Abstract

In the present paper, the steady two-dimensional temperature field in a plate subjected to highly localized volumetric heat generation is numerically investigated. The integral form of heat conduction equation is solved by using the concept of Control Volume Finite Element Method (CVFEM) which combines the ideas from Finite Element Method (FEM) and Finite Volume Method (FVM). In some literatures, it has been referred to as vertex-centered Finite Volume Method. The control volume mesh of CVFEM is built from the primary triangular mesh created by the same procedure for three-node triangular mesh generation as found in FEM. In contrast to the one-point integration scheme which used in conventional cell-centered Finite Volume Method, a multiple-point integration scheme is developed for more accurate integration of heat generation term. A square plate made of isotropic homogeneous material with boundary conditions of zero temperature along all edges is utilized as the solution domain. The effect of heat generation parameter and mesh arrangement, including structured and unstructured meshes, on the numerical solutions are observed. Furthermore, since this study does not attempt to solve the problem by using adaptive method, structured and unstructured meshes are provided by dividing the domain's boundary with uniform spacing. The spacing length depends on the mesh size requirement of each calculation. A non-dimensional error indicator for evaluating the accuracy of numerical solutions is also developed. The numerical results show that the saw-tooth temperature contours can be noticed in high thermal gradient zone, close to the central of the plate. The wavy temperature contours revealing the inaccuracy of numerical results can be reduced by using either fine unstructured mesh, multiple-point integration scheme or both.

Keywords*:* Control volume finite element method, heat transfer, non-uniform heat generation.

1. Introduction

Many applications in engineering practice involve the heat transfer analysis of solid body subjected to internal heat generation including nuclear fission in fuel elements of nuclear reactors, chemical reaction taking place within the solid body or the passage of electric current through the solid. Several researchers developed the numerical procedures for solving this heat transfer problem such as Boundary Element Method (BEM) and Finite Element Method (FEM).

The BEM techniques for heat conduction problem with internal heat source have been proposed in literatures during last decade. Shiah and Lin [1] presented a multiple reciprocity BEM formulation for analyzing the thermoelasticity of anisotropic plate subjected to thermal loading due to the internal volumetric heat source under steady state. Several forms of non-uniform heat generation rate were employed to test their methodology by comparing their results with the FEM results. Mohammadi et al. [2] reported the BEM results for the unsteady heat conduction problem involving non-homogeneous and time-dependent heat source. Various heat sources such as time-independent non-uniform heat source, time-dependent non-uniform heat source and temperature-dependent heat source were tested by their BEM technique. Although BEM offers advantage over FEM including the smaller matrix size due to the reduced number of nodes, FEM receives more attention than BEM because of its simpler mathematical formulation.

Several investigations were performed by using FEM with adaptive technique. Bag et al. [3] used FEM to find the transient response of axisymmetric heat conduction in a plate subjected to heating from laser beam in laser welding application. The adaptive finite element result was reported for the intense highly localized surface heating problem in square plate [4-5]. In afore-mentioned articles, the use of highly localized refined meshes is required for accurate temperature fields. The adaptive remeshing technique is utilized in [4-5] to generate unstructured mesh which provides the small elements in the regions that the temperature changes is large whereas the large elements are placed in the regions that temperature change is small. To avoid using the special computational technique cited above, a numerical procedure is developed.

The numerical method used in this work is the control volume finite element method (CVFEM). Sometimes, CVFEM is referred to as the vertex-based finite volume method which is a type of finite volume method (FVM) which the nodal points are first defined and then the control volumes are constructed around them. The brief introduction to CVFEM concept, discretization of governing equation and solution procedure will be found in section 2. Besides, the solution accuracy is further improved by changing the integration technique of heat generation term from the conventional one-point integration that was used in cell-centered finite volume method [8] to a new one called the multiple-point integration. Both integration schemes will be also mentioned in section 2. Section 3 describes the computational meshes for calculations and the criterion to evaluate the accuracy of numerical solutions. The numerical results are exhibited and discussed in section 4. Finally, section 5 presents the conclusions.

2. Mathematical formulation

2.1 Heat conduction equation

The heat conduction is simulated here by considering the two-dimensional steady heat flow through a square plate with isotropic and homogeneous properties. The governing equation for steady two-dimensional heat conduction can be written in Cartesian (x, y) coordinates as

$$k\left(\frac{\partial^2 T}{\partial x^2}+\frac{\partial^2 T}{\partial y^2}\right)+Q=0 \tag{1}$$

where T is the temperature, k is the material thermal conductivity and Q is the internal heat generation per unit volume. To find the solution, the appropriate boundary conditions have to be imposed on the domain's boundaries.

The common types of boundary condition for the heat conduction analysis are available such as (a) specified surface temperature, (b) specified heat flux on the surface, (c) specified surface heat convection and (d) specified surface heat radiation. Only the boundary condition type (a) is utilized in this paper.

2.2. Numerical method

In this section, the definition of control volume is firstly described. Next, the derivation of discretized equation is given. Finally, the solution procedure for numerical calculations is outlined.

2.2.1 Domain discretization

The computational domain is subdivided into a finite number of contiguous control volumes by a numerical grid. The grid nodes define vertices of control volumes. They are built from the triangular grid that can be constructed from mesh generation subroutine available in FEM commercial code or independent pre-processor software. Fig. 1 exhibits the polygonal control volume and triangular meshes which their typical meshes are filled by the light-blue and light-green, respectively. A polygonal control volume around each node is constructed by joining the centers of neighboring triangular elements to corresponding sides of those elements.

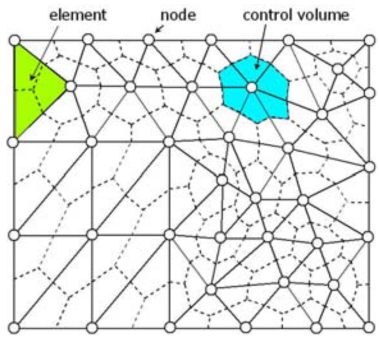

Fig.1 Control volume and triangular meshes

2.2.2 Control volume finite element method

The key step of CVFEM is the integration of Eq. (1) over a two-dimensional control volume (CV) yielding

$$\int\left(k\left(\frac{\partial^2 T}{\partial x^2}+\frac{\partial^2 T}{\partial y^2}\right)+Q\right)dV=0 \cdot \tag{3}$$

The volume integrals in the first parenthesis on the left hand side are rewritten as integrals over the entire bounding surface of the control volume by using Gauss' divergence theorem [7]. Eq. (3) can be rewritten in the following form:

$$\int\left(\left(k\frac{\partial T}{\partial x}\right)n_x+\left(k\frac{\partial T}{\partial y}\right)n_y\right)dA+\int QdV=0 , \tag{4}$$

where n_x and n_y are the direction cosines of unit vector of entire surface bounding control volume (CS) in x and y directions, respectively. The surface integral on the left hand side of Eq. (4) is evaluated by midpoint-rule as

$$\int\left(\left(k\frac{\partial T}{\partial x}\right)n_x+\left(k\frac{\partial T}{\partial y}\right)n_y\right)dA = \sum_{i=1}^{NI}\left\{\left(k\frac{\partial T}{\partial x}n_x+k\frac{\partial T}{\partial y}n_y\right)_i \Delta A_i\right\}, \tag{5}$$

where ΔA is the face area defined as a portion of entire surface bounding control volume and subscripts i counts the number of faces from 1 to NI. The temperature gradients at the faces can be computed by using the shape functions [8-9],

$$\frac{\partial T}{\partial x}=\sum_{k=1}^{3}\frac{\partial N_k}{\partial x}T_k , \quad \frac{\partial T}{\partial y}=\sum_{k=1}^{3}\frac{\partial N_k}{\partial y}T_k , \tag{6}$$

where k = 1, 2, 3; and N_k represent the shape functions of linear triangular elements.

The volume integral of internal heat generation is approximated by mid-point rule,

$$\int QdV = Q_P V_P , \tag{7}$$

where Q_P is the internal heat generation rate computed at the node P and V_P is the volume of the control volume surrounding node P. This scheme is referred to as one-point integration (CVFEM-OP) and shown in Fig. 2(a). Its counterpart, multiple-point integration (CVFEM-MP), is illustrated in Fig. 2(b).

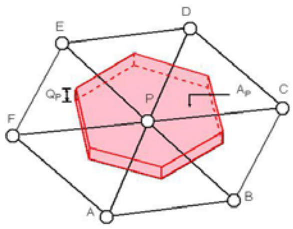

(a)

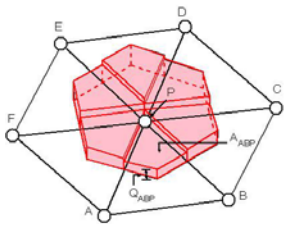

(b)

Fig.2 Numerical integration schemes for heat generation term: (a) CVFEM-OP, (b) CVFEM-MP

In CVFEM-MP, the volume integral of internal heat generation is evaluated by changing the whole integration over the control volume into the summation of integrations over sub-control volumes. In Fig. 2(b), the typical sub-control volumes such as ABP, BCP, CDP, DEP, EFP and FAP are shown. The individual integration in sub-control volume is computed by mid-point rule. The integral in sub-control volume is calculated by multiplying the heat generation value at the center of sub-control volume by the volume of that sub-control volume. The concept of CVFEM-MP may be written as

$$\int QdV = \sum_{m=1}^{NE} Q_m V_m , \tag{8}$$

where Q_m is the internal heat generation at the center of sub-control volume and the subscript m counts the number of sub-control volumes from 1 to NE.

2.2.3 Solution procedure

The discretized equations for the temperature of all control volumes of CVFEM-OP are obtained by substituting Eqs. (5), (6) and (7) into Eq. (4). Slightly different from CVFEM-OP approach, the discretized equations for CVFEM-MP are gained by substituting Eqs. (5), (6) and (8) into Eq. (4). Next, the system of algebraic equations are incorporated with boundary conditions and solved by using the matrix-free Gauss-Seidel point-by-point iterative solver. The stability of numerical solutions is also enhanced by using the under-relaxation parameter of 0.5. The iteration is terminated when the tolerance is less than 10^{-6}.

3. Problem of interest

In Fig. 3, a square plate with 0.01 m thickness where all edges are constrained to a constant temperature T=0°C. The spatial domain is defined by (0≤x≤1 m, 0≤y≤1 m). The plate has thermal conductivity k = 1 W/(m.K) and generates volumetric heat Q as follows

$$\begin{aligned}\frac{Q}{k} &= 2y(1-y)\left[\tan^{-1}\beta - \frac{\alpha(1-2x)}{\sqrt{2}(1+\beta^2)} + \frac{\alpha^2\beta x(1-x)}{2(1+\beta^2)^2}\right] + \\ &\quad 2x(1-x)\left[\tan^{-1}\beta - \frac{\alpha(1-2y)}{\sqrt{2}(1+\beta^2)} + \frac{\alpha^2\beta y(1-y)}{2(1+\beta^2)^2}\right]\end{aligned} \tag{9}$$

where

$$\beta = \alpha\left(\frac{x+y}{\sqrt{2}} - 0.8\right) \tag{10}$$

and α is the parameter that controls the intensity of heat sink and heat source in addition to the distribution of heat generation in the plate. The analytical temperature is given as

$$T = xy(1-x)(1-y)\tan^{-1}\beta \quad (11)$$

The analytical temperature distributions for $\alpha = 50$ and $\alpha = 100$ are shown in Figs. 4(a) – 4(b), respectively. In Figs. 4(c) – 4(d), the internal volumetric heat generation profiles along s coordinate for $\alpha = 50$ and $\alpha = 100$ are respectively illustrated.

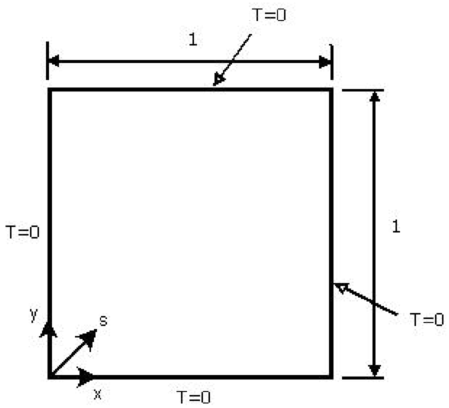

Fig. 3 Geometry, coordinates, and boundary conditions for heat conduction in a square plate.

3.1 Computational mesh

In this work, two types of triangulation patterns are selected for numerical calculations including structured and unstructured meshes. The summary of the number of nodes and elements in all computational meshes is shown in Table 1. Six levels of mesh size are employed for the numerical calculations. The first three levels are used for the case of $\alpha = 50$ while the last three levels are used for the case of $\alpha = 100$. For the comparison purpose, the number of nodes in unstructured mesh (USM) is selected as close as possible to the number of nodes in structured mesh (SM) under the same level of mesh size such as SM1 and USM1. Figs. 5 and 6 exhibit the shape of triangular elements and distribution of nodal points of computational meshes both structured and unstructured.

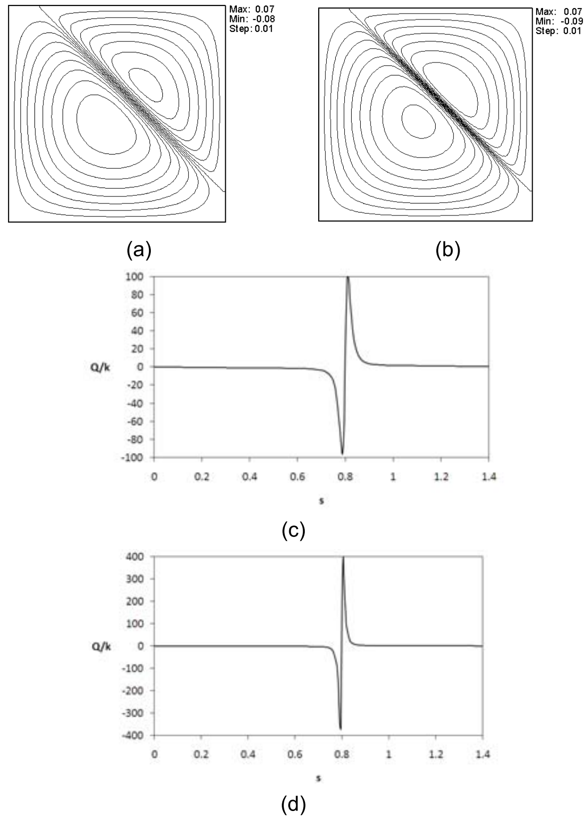

Fig. 4 (a) analytical temperature contours for $\alpha = 50$ (b) analytical temperature contours for $\alpha = 100$ (c) volumetric heat generation distribution along s coordinate for $\alpha = 50$ (d) volumetric heat generation along s coordinate for $\alpha = 100$.

Table 1 Total number of nodes (N) and total number of elements (E) in structured mesh (SM) and unstructured mesh (USM)

Mesh	N	E	Mesh	N	E
SM1	961	1800	USM1	936	1762
SM2	1681	3200	USM2	1239	2348
SM3	2601	5000	USM3	2423	4664
SM4	3721	7200	USM4	3583	6944
SM5	5041	9800	USM5	4751	9248
SM6	6561	12800	USM6	5944	11602

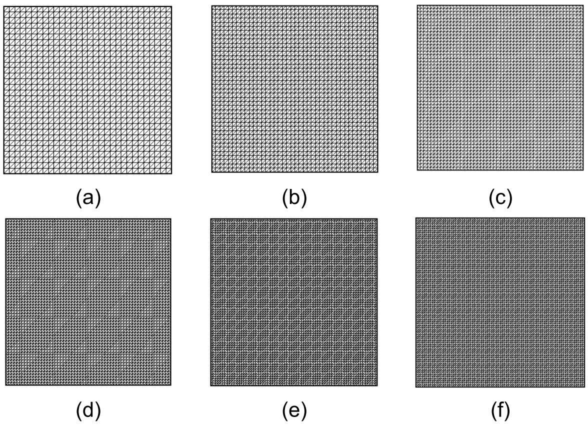

Fig. 5 The computational grids of (a) SM1, (b) SM2, (c) SM3, (d) SM4, (e) SM5, and (f) SM6

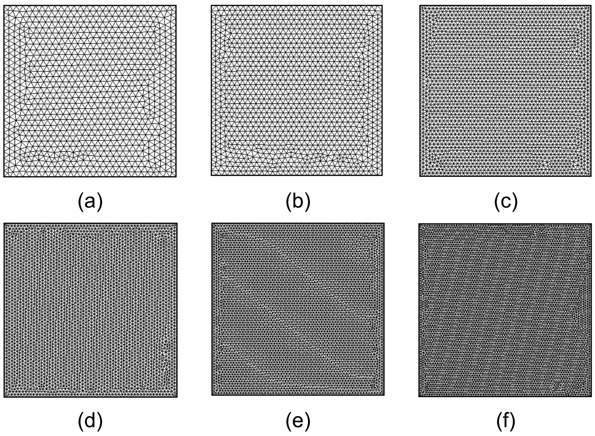

Fig. 6 The computational grids of (a) USM1, (b) USM2, (c) USM3, (d) USM4, (e) USM5, and (f) USM6

3.2 Error evaluation

A non-dimensional error measure, E, is defined for assessing the numerical accuracy of numerical solution as follows

$$E = \left(\sum_j \left|T_j^A - T_j^N\right|\right) \Big/ \left(\sum_j \left|T_j^A\right|\right) \times 100\% \qquad (12)$$

where the superscripts A and N imply the analytical and numerical solutions, respectively; the subscript j counts the number of nodal points in the domain.

4. Results and discussion

In the present paper, the analytical and CVFEM results are compared to evaluate the accuracy of the CVFEM results. The effect of mesh size, heat generation parameter (α), numerical scheme for integration of volumetric heat generation, and the mesh pattern on the accuracy of CVFEM results are reported.

For structured mesh and $\alpha = 50$, Figs. 7(a) - 7(c) show the effect of mesh size on the CVFEM-OP and CVFEM-MP results. The temperature contours obtained from the coarse mesh SM1 is worse than those from the fine mesh SM3 especially along the diagonal course from upper left to lower right of the plate. The zigzag of contour lines in that area can be observed. The area of wavy contours is large when the coarse mesh is used. Therefore, the numerical accuracy can be improved by using small mesh size.

For structured mesh and $\alpha = 100$, the area of wavy contours is very small as demonstrated in Figs. 7(d) – 7(f). The temperature gradient in this area is very high. To obtain the same accuracy as the numerical results for $\alpha = 50$, the required mesh size for $\alpha = 100$ is smaller. Another way that can be used to display the numerical error from numerical methods is the temperature profiles along s direction [4-5] as illustrated in Fig. 8. As seen in the Figs. 7 - 8, the CVFEM-MP results are more accurate than the CVFEM-OP results.

The integration error of heat generation term from mid-point rule of traditional FVM can be successfully reduced by using the CVFEM-MP. Fig. 9 shows that this concept can be applied with unstructured mesh. The errors of CVFEM-OP and CVFEM-MP results are summarized in Table 2.

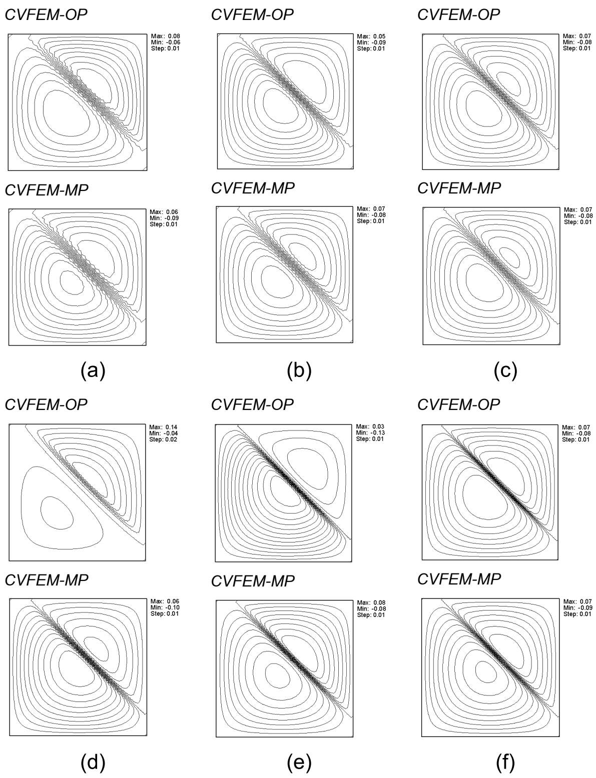

Fig. 7 Effect of mesh size and α on the CVFEM results with structured mesh (a) SM1, $\alpha = 50$, (b) SM2, $\alpha = 50$, (c) SM3, $\alpha = 50$, (d) SM4, $\alpha = 100$, (e) SM5, $\alpha = 100$,and (f) SM6, $\alpha = 100$

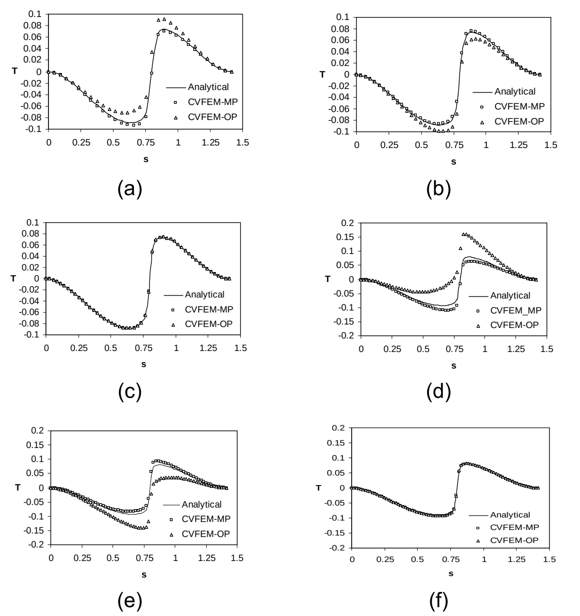

Fig. 8 Temperature distribution along s coordinate with structured mesh (a) SM1, $\alpha = 50$, (b) SM2, $\alpha = 50$, (c) SM3, $\alpha = 50$, (d) SM4, $\alpha = 100$, (e) SM5, $\alpha = 100$,and (f) SM6, $\alpha = 100$

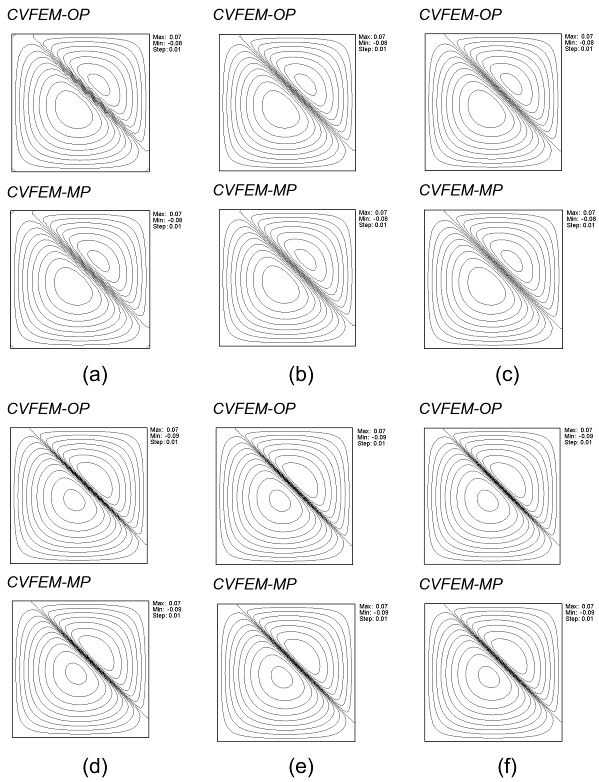

Fig. 9 Effect of mesh size and α on the CVFEM results with unstructured mesh (a) USM1, $\alpha = 50$, (b) USM2, $\alpha = 50$, (c) USM3, $\alpha = 50$, (d) USM4, $\alpha = 100$, (e) USM5, $\alpha = 100$,and (f) USM6, $\alpha = 100$

Table 2 Error of numerical results

α	Mesh	$E_{CVFEM\text{-}OP}$	$E_{CVFEM\text{-}MP}$
50	SM1	22.13%	5.31%
	SM2	12.16%	2.99%
	SM3	1.02%	0.24%
	USM1	2.03%	0.64%
	USM2	1.13%	0.46%
	USM3	0.47%	0.23%
100	SM4	70.39%	16.45%
	SM5	45.19%	10.94%
	SM6	1.05%	0.34%
	USM4	1.47%	0.30%
	USM5	0.47%	0.22%
	USM6	0.37%	0.19%

5. Conclusions

The finite volume analysis for steady heat conduction in a square plate subjected to non-uniform volumetric heat generation is performed. The method employed here based on the concept of control volume finite element method and the multiple-point integration for the heat generation term of heat conduction equation called CVFEM-MP. The effect of mesh size, heat generation parameter, mesh pattern and the numerical integration scheme on the temperature distribution in the plate are defined. CVFEM-MP results are better than CVFEM with the one-point integration for the heat generation term (CVFEM-OP) in all cases of interest. CVFEM-MP results converge to the analytical results with small number of nodes. Furthermore, the calculations on unstructured mesh give more accurate results than the calculations on structured mesh.

References

[1] Shiah, Y.C. and Lin, Y.J. (2003). Multiple reciprocity boundary element analysis of two-dimensional anisotropic thermoelasticity involving an internal arbitrary non-uniform volume heat sources. *International Journal of Solids and Structures*, Vol. 40, pp. 6593-6612.

[2] Mohammadi, M., Hematiyan, M.R. and Marin, L. (2010). Boundary element analysis of nonlinear transient heat conduction problems involving non-homogeneous and nonlinear heat sources using time-dependent fundamental solutions. *Engineering Analysis with Boundary Elements*, Vol. 34, pp. 655-665.

[3] Phongthanapanich, S., Traivivatana, S., Boonmaluth, P. and Dechaumphai, P. (2006). Nodeless variable finite element method for heat transfer analysis by means of flux-based formulation and mesh adaptation. *Acta Mech Sinica*, Vol. 22, pp. 138-147.

[4] Phongthanapanich, S. and Dechaumphai, P. (2008). Adaptive nodeless variable finite elements with flux-based formulation for thermal-structure analysis. *Acta Mech Sinica*, Vol. 24, pp. 181-188.

[5] Bag, S., Trivedi, A. and De, A. (2009). Development of a finite element based heat transfer model for conduction mode laser spot welding process using an adaptive volumetric heat source. *International Journal of Thermal Sciences*, Vol. 48, pp. 1923-1931.

[6] Lertsurayut, T. and Maneeratana, K. (2002). The utilization of Delaunay triangulation in finite volume modeling, paper presented in *the 16th Conference of Mechanical Engineering Network of Thailand*, Phuket, Thailand.

[7] Versteeg, H.K. and Malalasekera, W. (1995). An introduction to computational fluid dynamics: The finite volume method, Longman, England.

[8] Baliga, B.R. and Patankar, S.V. (1988). Elliptic systems: Finite element I. *Handbook of Numerical Heat Transfer*, Wiley, New York.

[9] Reddy, J.N. (1993). An Introduction to the Finite Element Method, McGraw-Hill, New York.